

## INFLUENCE OF LOADING RATE ON THE FRACTURE BEHAVIOUR OF NATURAL HYDRAULIC AND AERIAL LIME MORTARS

XIAOXIN ZHANG<sup>\*\*†</sup>, LUCÍA GARIJO<sup>†</sup>, GONZALO RUIZ<sup>†</sup> AND JOSÉ J. ORTEGA<sup>†</sup>

<sup>†</sup> Universidad de Castilla-La Mancha (UCLM)

Avda. Camilo José Cela s/n, 13071 Ciudad Real, Spain

\*e-mail: Xiaoxin.Zhang@uclm.es, zhangxiaoxinhrb@gmail.com

**Keywords:** Natural hydraulic lime mortar, Aerial lime mortar, Fracture energy, Loading rate, Dynamic Increase Factor.

**Abstract:** Natural hydraulic and aerial lime mortars are used extensively for restoration works due to their good compatibility with the substrate material in historical masonry construction. Recently, the study of the influence of loading rate of such materials is getting more attention due to the fact that many historic masonry structures are situated in zones of seismic activity. However, the references are still scarce in comparison to that of steel and concrete and the studies focused on the measurement of the influence of loading rate on the fracture energy are limited, although it is an important parameter to characterize the ductility and the fracture behaviour of the material. Thus, in the paper, an aerial and a natural hydraulic lime mortar specimens were tested at various loading rates (loading-point displacement rates) from the quasi-static one,  $5.0 \times 10^{-4}$  mm/s, to rate sensitive ones,  $5.0 \times 10^{-1}$  mm/s and  $1.6 \times 10^1$  mm/s. For this purpose, it was used a servo-hydraulic testing machine up to its maximum range of velocities. The results show that the fracture energy and the peak load of both lime mortars are rate sensitive. The maximum dynamic increase factors of the fracture energy are 1.9 for both mortars, while 1.4 and 1.6 for the natural hydraulic and the aerial lime mortars, respectively, in the peak load. This behaviour is related to viscous effects of free water in the mortar.

### 1 INTRODUCTION

Lime mortars, both hydraulic and aerial, are present in many historical constructions as masonry joints and/or renders. From a structural point of view, it is relevant their function as joints in walls [1]. It is also important their use for restoration purposes as repointing, grout injections, consolidations, etc. due to their good compatibility with the substrate material.

Considering their large use in historical masonry constructions, lime mortars are often subjected to dynamic loads, such as earthquakes, impacts or wind gusts. However, their characterization under such conditions is not studied as much as for other materials such

as steel [2] and concrete [3].

In this concern, Pereira and Lourenço [4] tested a commercial pre-mixed mortar under different strain rates ranging from  $2 \text{ s}^{-1}$  to  $200 \text{ s}^{-1}$  by using a drop-weight tower. For the highest strain rate, they obtained a dynamic increase factor (DIF), a ratio of the dynamic response over the quasi-static one, for the fracture energy in compression of 2.73. They compared the deformations obtained through strain gages and a high speed camera and checked that the results were similar measured with both methods. Asprone *et al.* [5] characterized a natural hydraulic lime mortar reinforced with basalt fibers in tension under medium and high strain-rates with a Hydro-

pneumatic machine and a Hopkinson bar, respectively. They obtained a DIF of 5.1 for a strain rate of  $90 \text{ s}^{-1}$ .

For bending behaviour, Chan and Bindiganavile [6] analyzed the strain rate sensitivity of plain and fiber-reinforced hydraulic lime mortars at strain rate range of  $10^{-6}$  to  $10 \text{ s}^{-1}$  by using a universal testing machine and a drop-weight impact machine. For plain mortar, the results show that the DIF for the modulus of rupture was 12 at a strain rate of  $10 \text{ s}^{-1}$ , while it was 53 for fracture toughness. Moreover, Bindiganavile *et al.* [7, 8] studied the bond behaviour between the stone masonry block and the plain and fiber-reinforced hydraulic lime mortar. They observed an improvement of the bond strength due to the polypropylene micro-fibers.

However, the studies concerning the rate effect on lime mortars are scant, especially for fracture energy, despite being an important parameter to characterize the ductility and fracture behaviour of the material. Thus, the objective of this research is to characterize the response of two lime mortars, one hydraulic and another aerial, in flexion under three different loading rates, from quasi-static ones,  $5.0 \times 10^{-4} \text{ mm/s}$  to rate dependent ones,  $5.0 \times 10^{-1} \text{ mm/s}$  and  $1.6 \times 10^1 \text{ mm/s}$ . The results show that the peak load and the fracture energy increase with the loading rate. Moreover, the equations of the loading rate behaviour for the fracture energy and the peak load are obtained, which could be useful for the numerical simulations of lime mortars under dynamic loads.

The paper is structured as follows: the experimental procedure is presented in Section 2, in Section 3 the results and discussion are shown. Finally, in Section 4 some conclusions are depicted.

## 2 EXPERIMENTAL PROCEDURE

### 2.1 Raw materials

It was used two types of lime according to EN 459-1 [9]: a natural hydraulic one of class NHL 3.5, supplied by “Socli Italcementi Group” (France), and an aerial one of class CL

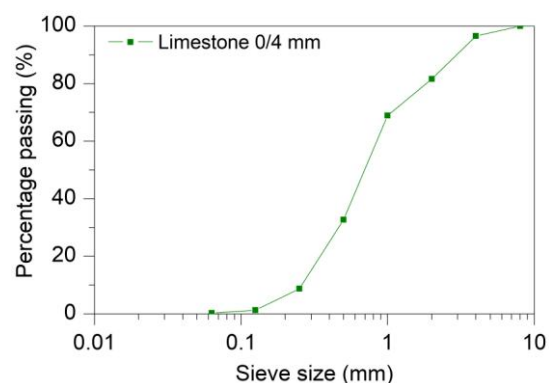


**Figure 1:** Particle size distribution curve of the aggregate used.

90-S from “Calcasa Calciner” (Spain). The aggregate was a crushed limestone sand with particle size distribution as shown in Figure 1.

### 2.2 Mortar composition and preparation

Two lime mortars were fabricated with corresponding limes, one aerial and another hydraulic. The lime/aggregate ratio used for both mortars was of 1:3 by volume and the water/lime ratio was of 0.9 also by volume. Volume proportions were converted into weight to avoid imprecision in the measuring process.

The specimens were prisms of  $40 \times 40 \times 160 \text{ mm}^3$ , in accordance to EN 1015-11 [10]. The ones of natural hydraulic lime mortar were kept in the humid chamber under conditions ( $\text{RH } 95 \pm 5\%$  and  $20 \pm 2^\circ\text{C}$ ) and the specimens of aerial lime mortar were in storage for seven initial days in the humid chamber and the rest under ambient laboratory conditions ( $\text{RH } 50 \pm 10\%$  and  $22 \pm 3^\circ\text{C}$ ).

### 2.3 Experimental procedure

The flexural and compressive strengths were measured at 56 days on prisms and semi-prisms, respectively, according to EN 1015-11 [10]. For such a purpose, it was used an Instron 1011 testing machine and the procedures of previous works [1, 11] were followed.

#### 2.3.1 Three-point bending tests

The fracture energy was measured through three-point bending tests by adapting the

procedure of RILEM [12] and the improvements proposed by Planas, Guinea and Elices [13-15]. The tests were performed at 56 days on three specimens with a precast notch at mid span up to half depth measuring  $40 \times 40 \times 160 \text{ mm}^3$ . It was used an Instron 8805 testing machine and the procedure described in previous works [1, 11] were followed. That is to say, the weight compensation technique was applied during the test, anti-torsion supports that permit rotation out of the plane of the specimen were used and two LVDT (linear variable differential transducers) were placed to measure the displacements of the specimen. Finally, the corrections of the load-displacement curve were applied. The tests were performed in displacement control at three different loading rates. The slowest test was performed at a rate of  $5.0 \times 10^{-4} \text{ mm/s}$  up to a displacement of 0.3 mm and at  $2.5 \times 10^{-3} \text{ mm/s}$  during the rest of the test (up to a displacement of 3 mm). The following ones were performed at rates of  $5.0 \times 10^{-1}$  and  $1.6 \times 10^1 \text{ mm/s}$ , respectively for the entire test. Thus, the slowest test lasted around 30 minutes and the fastest around 0.3 seconds.

### 3 RESULTS AND DISCUSSION

#### 3.1 Experimental results

The mechanical properties at the quasi-static regime for both lime mortars are shown in Table 1, where  $f_{flex}$  and  $f_c$  are, respectively, the flexural and compressive strengths. The values in parenthesis are the corresponding standard deviations.

**Table 1:** Results of mechanical properties at the quasi-static regime

Type of lime mortar	$f_{flex}$ (MPa)	$f_c$ (MPa)
Hydraulic	1.1 (0.1)	3.1 (0.2)
Aerial	0.54 (0.01)	1.30 (0.03)

The mechanical properties in the dynamic regime of both lime mortars are shown in Tables 2 and 3, respectively, where  $\delta$  is the loading rate in mm/s,  $P_{max}$  is the maximum load,  $DIF$  the dynamic increase factor as

mentioned in the Introduction,  $G_F$  the fracture energy and  $\dot{\epsilon}$  is the nominal strain rate obtained through Eq. 1.

$$\dot{\epsilon} = \frac{6(D-a)\delta}{S^2} \quad (1)$$

Where  $D$ ,  $a$  and  $S$  are the depth, notch depth and span between supports, respectively of the specimen in the three-point bending test. In a similar way, the values in parenthesis are the standard deviations.

**Table 2:** Mechanical properties under different loading rates for the natural hydraulic lime mortar

$\delta$ (mm/s)	$P_{max}$ (N)	$DIF$ $P_{max}$	$G_F$ (N/m)	$DIF$ $G_F$	$\dot{\epsilon}$ ( $s^{-1}$ )
$5.0 \times 10^{-4}$	99 (10)	1.0	12.2 (1)	1.0	$6 \times 10^{-6}$
$5.0 \times 10^{-1}$	120 (10)	1.2	17.3 (1)	1.4	$6 \times 10^{-3}$
$1.6 \times 10^1$	140 (15)	1.4	22.8 (10)	1.9	$2 \times 10^{-1}$

**Table 3:** Mechanical properties under different loading rates for the aerial lime mortar

$\delta$ (mm/s)	$P_{max}$ (N)	$DIF$ $P_{max}$	$G_F$ (N/m)	$DIF$ $G_F$	$\dot{\epsilon}$ ( $s^{-1}$ )
$5.0 \times 10^{-4}$	21 (4)	1.0	3.0 (1)	1.0	$6 \times 10^{-6}$
$5.0 \times 10^{-1}$	26 (3)	1.2	4.0 (1)	1.3	$6 \times 10^{-3}$
$1.6 \times 10^1$	32 (2)	1.5	5.7 (1)	1.9	$2 \times 10^{-1}$

Figures 2 and 3 show the load-displacement curves of the natural hydraulic and the aerial lime mortars, respectively. In both, it is observed that the peak load increases for higher loading rates. Concerning the stiffness, the same tendency is shown.

Furthermore, in Figures 4 and 5 it is observed graphically that the peak load and fracture energy increase, respectively for both mortars, with increasing loading rates. This phenomenon could be due to viscous effects originated by the presence of free water in voids and due to crack propagation effects. That is to say, due to the fact that at lower loading rates, the cracks propagate more slowly than at higher loading rates, when the cracks propagate faster and in a more straight way. The dynamic increase factors for the

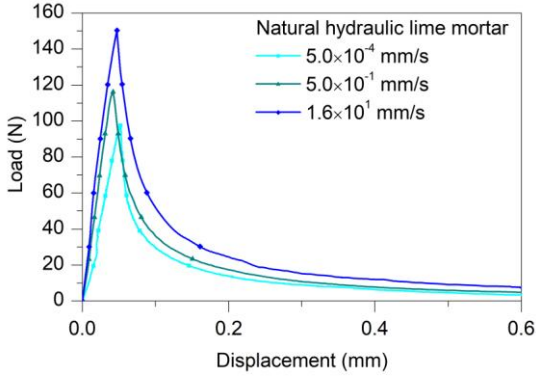


**Figure 2:** Load-displacement curves for the natural hydraulic lime mortar.

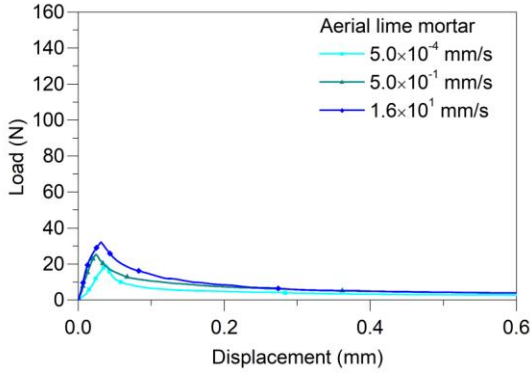


**Figure 3:** Load-displacement curves for the aerial lime mortar.

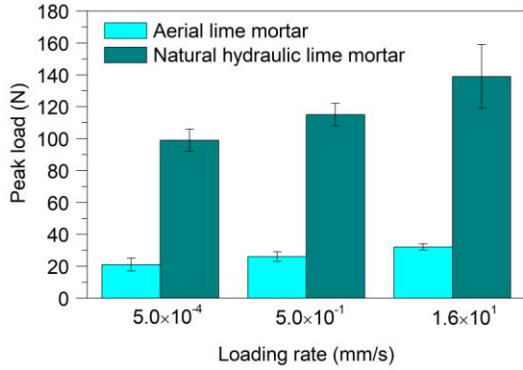


**Figure 4:** Peak load evolution with the loading rates for both lime mortars.

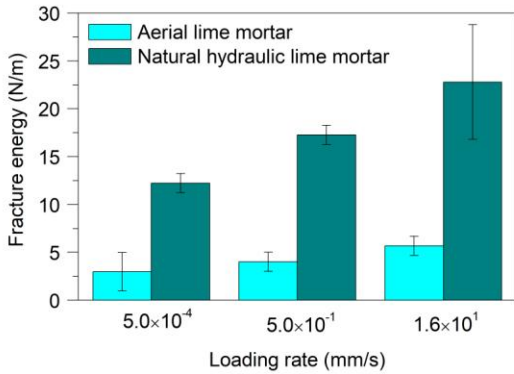


**Figure 5:** Fracture energy evolution with the loading rates for both lime mortars.

highest loading rate are 1.4 and 1.6 in the peak load, respectively for the natural hydraulic and the aerial lime mortars and 1.9 in the fracture energy for both.

Finally, in Figures 6 and 7 it is shown the rate dependence tendencies for the peak load and the fracture energy, respectively, of the natural hydraulic and the aerial lime mortars. These relationships are given by Eqs. 2-3 and corresponding coefficients of Table 4. They could be useful for the numerical simulations of lime mortars in the dynamic regime.

$$DIF_{P_{max}} = 1 + m \left( \frac{\dot{\delta}}{\dot{\delta}_0} \right)^n \quad (2)$$

$$DIF_{G_F} = 1 + p \left( \frac{\dot{\delta}}{\dot{\delta}_0} \right)^q \quad (3)$$

where  $DIF_{P_{max}}$  and  $DIF_{G_F}$  are, respectively, the dynamic increase factors of the peak load and the fracture energy,  $\dot{\delta}$  is the loading rate in mm/s and  $\dot{\delta}_0$  is equal to 1 mm/s.

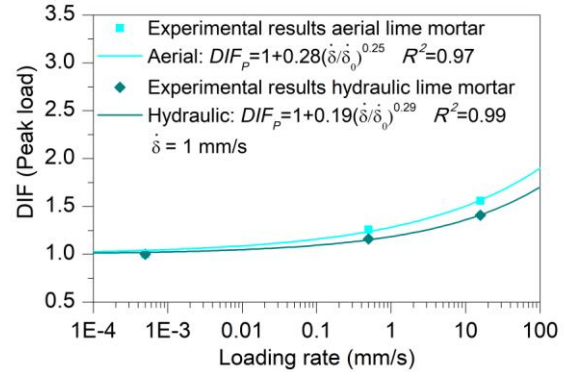


**Figure 6:** Loading rates dependence laws for the peak load in both lime mortars.

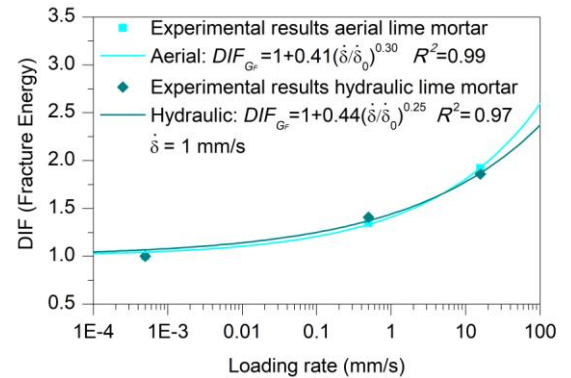


**Figure 7:** Loading rates dependence laws for the fracture energy in both lime mortars.

**Table 4:** Coefficients of Eqs. 2-3.

Type of lime mortar	$m$	$n$	$p$	$q$
Hydraulic	0.19	0.29	0.44	0.25
Aerial	0.28	0.25	0.41	0.30

#### 4 CONCLUSIONS

This research presents the loading rate effect on one hydraulic and an aerial lime mortars. The specimens were tested under three different loading rates, from  $5.0 \times 10^{-4}$  mm/s to  $1.6 \times 10^1$  mm/s. The results show that the peak load and the fracture energy increase with increasing loading rates. This is mainly due to the presence of water in voids and effects of crack propagation.

Finally, empirical equations for the rate sensitivity have been obtained for the peak load and fracture energy, which could be useful for the numerical simulations of lime mortars under dynamic regimes.

#### ACKNOWLEDGEMENTS

The authors acknowledge the program INCRECYT and the *Ministerio de Ciencia, Innovación y Universidades*, Spain, for the grant BIA2015-68678-C2-1-R and for the research project RTC-2017-6736-3.

#### REFERENCES

- [1] Garijo L, Zhang XX, Ruiz G, Ortega JJ, Yu RC, 2017. Advanced mechanical characterization of NHL mortars and cohesive simulation of their failure behaviour. *Construction and Building Materials*. **153**:569-77.
- [2] Cadoni E, Fenu L, Forni D, 2012. Strain rate behaviour in tension of austenitic stainless steel used for reinforcing bars. *Construction and Building Materials*. **35**:399-407.
- [3] Zhang XX, Abd Elazim AM, Ruiz G, Yu RC, 2014. Fracture behaviour of steel fibre-reinforced concrete at a wide range of loading rates. *International Journal of Impact Engineering*. **71**:89-96.
- [4] Pereira JM, Lourenço PB, 2017. Experimental characterization of masonry and masonry components at high strain rates. *Journal of Materials of Civil Engineering*. **29**(2):1-10.
- [5] Asprone D, Cadoni E, Iucolano F, Prota A, 2014. Analysis of the strain-rate behaviour of a basalt fiber reinforced natural hydraulic mortar. *Cement & Concrete Composites*. **53**:52-8.
- [6] Chan R, Bindiganavile V, 2010. Toughness of fibre reinforced hydraulic lime mortar. Part-2: Dynamic response. *Materials and Structures*. **43**(10):1445-55.
- [7] Islam MT, Bindiganavile V, 2014. Dynamic Fracture Toughness of Sandstone Masonry Beams Bound with Fiber-Reinforced Mortars. *Journal of Materials in Civil Engineering*. **26**(1):125-33.
- [8] Islam MT, Chan R, Bindiganavile V, 2012. Stress rate sensitivity of stone masonry units bound with fibre reinforced hydraulic lime mortar. *Materials and Structures*. **45**(5):765-76.
- [9] BS EN 459-1, 2015. Building lime – Part 1: Definitions, specifications and conformity criteria. Brussels, Belgium: BSI. p. 52.
- [10] BS EN 1015-11, 1999/A1:2006. Methods of test for mortar for masonry – Part 11: Determination of flexural and compressive strength of hardened mortar: BSI. p. 12.
- [11] Garijo L, Zhang XX, Ruiz G, Ortega JJ, Wu Z, 2018. The effects of dosage and production process on the mechanical and physical properties of natural hydraulic lime mortars. *Construction and Building Materials*. **169**:325-34.
- [12] RILEM TC 50-FMC, 1985. Determination of the fracture energy of mortar and concrete by means of the three-point bend tests on notched beams. *Materials and Structures*. **18**:285-90.
- [13] Elices M, Guinea GV, Planas J, 1992. Measurement of the fracture energy using three point bend tests. 3. Influence of cutting the  $P$ - $\delta$  tail. *Materials and Structures*. **25**:327-34.
- [14] Elices M, Guinea GV, Planas J, 1992. Measurement of the fracture energy using three-point bend tests. 1. Influence of experimental procedures. *Materials and Structures*. **25**:121-218.
- [15] Planas J, Elices M, Guinea GV, 1992. Measurement of the fracture energy using three point bend tests. 2. Influence of bulk energy dissipation. *Materials and Structures*. **25**:305-12.